nature neuroscience

Vesicular proteins exocytosed and subsequently retrieved by compensatory endocytosis are nonidentical

Martin Wienisch & Jurgen Klingauf

Upon exocytosis, synaptic vesicle proteins are released into the plasma membrane and have to be retrieved by compensatory endocytosis. When green fluorescent protein–labeled versions of the vesicle proteins synaptobrevin-2 and synaptotagmin-1 are overexpressed in rat hippocampal neurons, up to 30% are found on axonal membranes under resting conditions. To test whether and to what extent these plasma membrane–stranded proteins participate in exo-endocytic cycling, a new proteolytic approach was used to visualize the fate of newly exocytosed proteins separately from that of the plasma membrane–stranded ones. We found that both pools were mixed and that endocytosed vesicles were largely composed of previously stranded molecules. The degree of nonidentity of vesicular proteins exo- and endocytosed depended on stimulus duration. By using an antibody to the external domain of synaptotagmin-1, we estimated that under physiological conditions a few percent of vesicular proteins were located near the active zone, from where they were preferentially recycled upon stimulation.

Following neurotransmitter release, clathrin-mediated endocytosis is thought to be the major pathway for synaptic vesicle recycling[1–4]. Alternatively, a fast 'kiss and run' mechanism, whereby vesicles connect only briefly to the plasma membrane without full collapse[5–8], might retrieve vesicular components more efficiently. In addition, a slow pathway via large infoldings and endosomes[9] may contribute to recycling.

Most of our knowledge of the kinetics of stimulated endocytosis in synaptic boutons comes from experiments using the fluorescent vesicle marker FM1-43 (refs. 7,10–13) and synapto-pHluorin (spH), a fusion construct of the vesicle protein synaptobrevin/VAMP-2 with a pH-sensitive green fluorescent protein (GFP) variant[8,14,15]. However, neither technique allows us to distinguish between different molecular mechanisms of membrane retrieval.

When visualizing the redistribution of enhanced GFP (eGFP)-tagged clathrin in hippocampal boutons[16], it was found that stimulation leads to a transient increase of fluorescence in boutons, with decay kinetics notably similar to previous estimates of the endocytic time course. However, the increase in fluorescence is preceded by a long delay, suggesting that endocytosis during the first few seconds of continuing stimulation is not mediated by the slow ($\sim$10 s) formation of clathrin-coated pits[17,18]. The rate of endocytosis, however, is fastest for short stimuli[15]. One likely interpretation is that the early phase of endocytosis does not depend on clathrin, but is of the 'kiss and run' type.

An alternative explanation, however, could be a pool of preassembled 'ready to go' coats at the periphery of the active zone, supporting a first wave of endocytosis. Such a first wave of endocytosis, via coated vesicles and lasting for only 10 s, has been observed in the first reconstruction of the time course of synaptic endocytosis obtained from electron micrographs of frog neuromuscular junctions quick-frozen at different time points after stimulation[19].

What distinguishes both scenarios fundamentally is the molecular identity of vesicles exo- and endocytosed by the same stimulus. Maintaining molecular identity is the hallmark of a kiss and run type of mechanism, whereas nonidentity would be the essential feature and kinetic advantage of a preassembled pool at the periphery of the active zone.

Indeed, up to 30% of the synaptic vesicle protein spH is present on the external bouton membrane of transfected hippocampal neurons[20]. Immuno-electronmicroscopy has revealed that endogenous synaptobrevin is also present in the synaptic membrane, at a density that is only three times lower than that in synaptic vesicles under resting conditions[21]. Exocytosed spH and synaptobrevin-eGFP disperse into the axonal plasma membrane during synaptic stimulation[20,22], prompting the question of whether this stranded plasma membrane pool of spH participates in synaptic vesicle retrieval during exo- and endocytosis.

Here we tested whether the same molecules that are exocytosed are retrieved during compensatory endocytosis. We introduced a tobacco etch virus (TEV) protease cleavage site between the synaptobrevin and GFP moieties. This site is only accessible to external enzyme if this protein is in the plasma membrane. This TEV motif–containing spH (spH-TEV) behaved identically to the original spH. We found that mostly digested molecules were recycled during compensatory endocytosis—that is, synaptobrevin molecules deposited on the plasma membrane before digestion. Identical results were obtained with a synaptotagmin-1-pHluorin construct. We conclude that most recycling synaptic vesicles lose their protein complement during exocytosis. By using an antibody to the external domain of synaptotagmin-1, we

Department of Membrane Biophysics, Max-Planck-Institute for Biophysical Chemistry, Am Fassberg 11, D-37077 Goettingen, Germany. Correspondence should be addressed to J.K. (J.Klingauf@mpi-bpc.mpg.de).

Received 4 April; accepted 16 June; published online 16 July 2006; doi:10.1038/nn1739

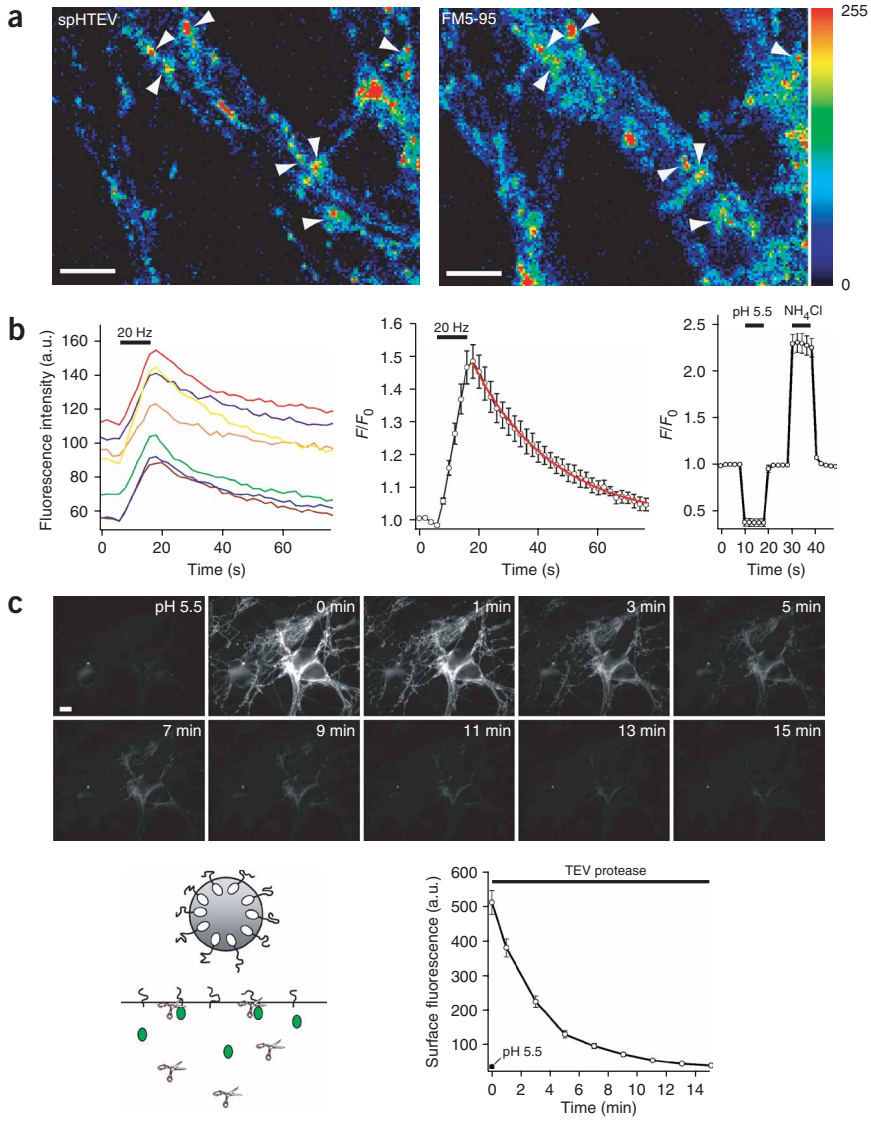

Figure 1 Synaptobrevin-TEV-pHluorin (spH-TEV) is targeted to functional boutons and the plasma membrane–stranded fraction can be effectively cleaved. (**a**) Axonal branches of hippocampal neurons in primary culture overexpressing spH-TEV. Difference image (left) obtained by subtraction of the picture recorded before from that recorded during a stimulation with 200 action potentials. Transient fluorescence increases at sites that can be stained and destained with the activity marker FM5-95 (right) identify them as functional presynaptic boutons. Scale bar, 5 μm. (**b**) Left, individual fluorescence transients of exemplar boutons marked by arrowheads in **a**; middle, average fluorescence signal (red line represents single exponential fit with $\tau = 26.9$ s); right, average fluorescence signal from boutons sequentially superfused with acidic solution (pH 5.5) and with ammonium chloride solution (50 mM). Comparing the size of the fluorescence change during the acidic pulse with the fluorescence change during the ammonium chloride pulse reveals that 33.2 ± 0.9% of spH-TEV are stranded in the plasma membrane ($n = 3$ experiments, >50 boutons each, error bars represent s.e.m.). (**c**) When neurons overexpressing spH-TEV were exposed to 0.12 U μl^{-1} TEV protease at room temperature, the pHluorin moiety was effectively cleaved, within 15 min, from molecules residing in the plasma membrane. Vesicular spH-TEV is inaccessible to the protease (bottom, left). This decreased the plasma membrane fluorescence down to a level comparable to that obtained with acidic solution (bottom, right). Scale bar, 10 μm.

estimated that under physiological conditions a small percentage of vesicular proteins are located near the active zone, constituting a pool of preferentially recycled molecules. A stimulus of 30–40 action potentials led to the compensatory endocytosis of about 5–10 vesicles, which is remarkably close to the number of vesicles in the readily releasable or docked pool of vesicles that are rapidly released by a similar number of action potentials (ref. 23).

RESULTS

Tracking the fate of vesicular proteins after fusion

Overall endocytic activity can be measured with spH, a fusion construct of the vesicle protein synaptobrevin and a pH-sensitive form (pHluorin) of GFP (ref. 15). The pHluorin in the acidic vesicle lumen is dequenched upon exocytosis, and reacidification of endocytosed vesicles is accomplished within about 5 s (ref. 24). Up to 30% of spH is present on the external axonal membrane of transfected hippocampal neurons (ref. 20 and **Fig. 1a**,**b**), regardless of the absolute level of spH expression.

To test whether synaptic vesicles maintain their identity with respect to their protein composition during exo-endocytic cycling, we introduced a TEV protease cleavage site between the VAMP and GFP moieties that is only accessible to external enzyme if spH-TEV is in the plasma membrane. Like spH, spH-TEV was specifically targeted to synaptic boutons. It colocalized with the synaptic activity marker FM5-95 (**Fig. 1a**), and fluorescence transients upon stimulation with 200 action potentials were indistinguishable from those obtained with spH (**Fig. 1b**). As found for spH, up to 30% of spH-TEV was found on the plasma membrane of boutons at rest, as revealed by fluorescence quenching by short superfusion with an acidic solution of pH 5.5 (**Fig. 1b** right, and first two images in **Fig. 1c**). For investigating the fate of vesicular SNAREs after fusion, the plasma membrane pool of spH-TEV, which normally masks the spatiotemporal dynamics of vesicular SNARES during stimulation, was almost completely fluorescently 'silenced' by exposure to TEV protease for 15 min (**Fig. 1c**).

Vesicular proteins are lost after fusion

When axons expressing spH-TEV were stimulated, postdigest boutons lit up as vesicular spH-TEV was dequenched upon vesicle fusion (**Fig. 2a**, left). For analysis of the spatiotemporal dynamics of vesicular spH-TEV, we created a maximum projection image in which each pixel contained the maximum value over all images in the stack at that particular pixel; we drew a line of interest (LOI) along an axonal stretch and for each image plotted the fluorescence along this LOI for a width of 3 pixels (615 nm) in a kymograph image (**Fig. 2a**, right). Superfusion with acidic (pH 5.5) solution after digestion revealed that most spH-TEV in the plasma membrane had been digested (some spH-TEV became stranded again during the protease washout period).

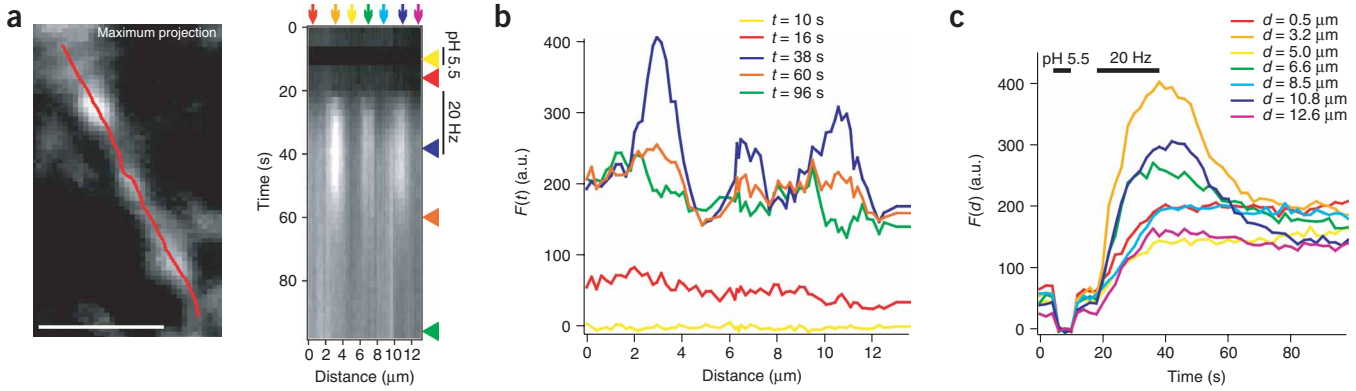

Figure 2 Vesicular proteins are lost after fusion. (**a**) Maximum projection image (left) of an axonal segment with three functional spH-TEV–expressing boutons stimulated with 400 action potentials. Scale bar, 5 μm. For further analysis, an LOI (red solid line) was placed along the axon to create a waterfall plot (right). Fluorescence intensities at each distance of the LOI (origin in upper left corner of maximum projection image) are integrated over a width (normal to the LOI) of three pixels. Vertical bars on the right indicate times of acidic pulse and stimulation. (**b**) Exemplar spatial profiles along the LOI in **a**, at different times indicated by arrowheads in **a**. (**c**) Exemplar time courses at different positions along the LOI in **a**, colorcoded according to the colors of arrows in **a**.

Upon stimulation, vesicular spH-TEV dequenched and, we were surprised to find, spread quickly in the axonal plasma membrane; this can be easily seen by comparing spatial (horizontal) and temporal (vertical) profiles of the kymograph at different times and distances (**Fig. 2b**,**c**). Because the fluorescence increase in axonal segments was not substantially delayed from the bouton signals (**Fig. 2c**), it is likely that vesicular SNARES diffuse rather freely in the plasma membrane. After stimulation, vesicular SNAREs were retrieved and quenched by endocytosis in the boutons only, with maybe some accumulation of exocytosed spH-TEV remaining at the periphery of the boutons at $t = 95$ s (**Fig. 2b**, compare blue and green profile).

Vesicular proteins exo- and endocytosed are not identical

Notably, recovery of the spH-TEV transients in the three boutons depicted appeared to be incomplete after digestion (**Fig. 2c**), as opposed to that of the transients before digestion (**Fig. 1b**). Thus, we next analyzed the recovery of fluorescence transients in a given set of boutons before and after digestion, upon stimulation with 100 action potentials (**Fig. 3**). Digestion with TEV protease increased the relative amplitude ($\Delta F/F_0$; that is, the change in fluorescence over initial fluorescence), as expected, but not the absolute amplitudes (**Supplementary Fig. 1** online), and indeed led to incomplete recovery (40.1% at 58 s after stimulus end) of fluorescence transients (**Fig. 3a**,**b**). Because vesicular proteins, once released, tend to diffuse away from the release sites (**Fig. 2**), a likely explanation is that during compensatory endocytosis, a portion of the plasma membrane–stranded spH-TEV has been retrieved, instead of the spH-TEV released during stimulation. Before digestion, plasma membrane–stranded spH-TEV will contribute equally to the dequenching signal during reacidification of endocytosed vesicles; however, after digestion, these stranded spH-TEV were fluorescently silent (**Fig. 3b**).

To test this hypothesis, we first restored the relative stoichiometry of molecules in the synaptic vesicles and the plasma membranes that had been subjected to proteolysis, by turning over the recycling pool of synaptic vesicles with a prolonged train of action potentials (800 action potentials at 5 Hz) in the same set of boutons and then stimulating again with 100 action potentials. Indeed, the transient nature of the spH signals was fully recovered (**Fig. 3c**). Thus, it seems that the majority of synaptic vesicles lose their molecular identity during exo- and endocytic cycling. Alternatively, our results can be explained if we assume that synaptic vesicles do indeed maintain their molecular identity in raft-like structures that diffuse slowly to the periphery of

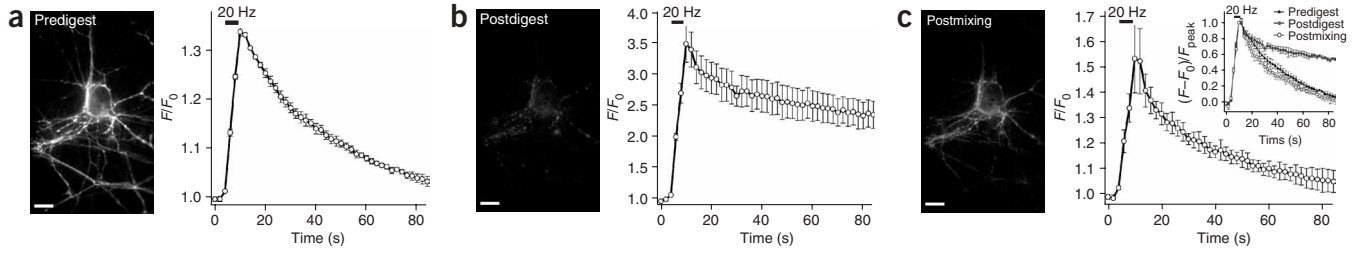

Figure 3 Vesicular proteins exo- and endocytosed during stimulation are not identical. (**a**) Left, image of axonal arborizations expressing spH-TEV before TEV protease digestion. Right, upon stimulation with 100 action potentials at 20 Hz, control fluorescence transients at boutons (shown in left image) recovered completely within 80 s after stimulation. (**b**) Left, image of axonal arborizations depicted in **a** after digestion with TEV protease; very little plasma membrane fluorescence was seen. Right, upon application of 100 action potentials at 20 Hz, the fluorescence transients of boutons (shown in left image) had increased relative amplitudes, as expected, but recovery was incomplete. (**c**) Left, image of axonal arborizations depicted in **a** after vesicle and plasma membrane pools of spH-TEV were mixed by using a prolonged train of action potentials (800 action potentials at 5 Hz); substantial fluorescence of plasma membrane–stranded spH-TEV was seen. Right, upon application of 100 action potentials at 20 Hz, fluorescence transients of boutons (image at left) again displayed complete recovery, demonstrating that endocytosis was not blocked by TEV protease digestion. Inset, normalized responses for 100 action potentials at 20 Hz, predigestion (**a**), postdigestion (**b**) and postmixing ($n = 3$ experiments, >50 boutons each, error bars represent s.e.m.). Scale bar in **a**–**c**, 10 μm.

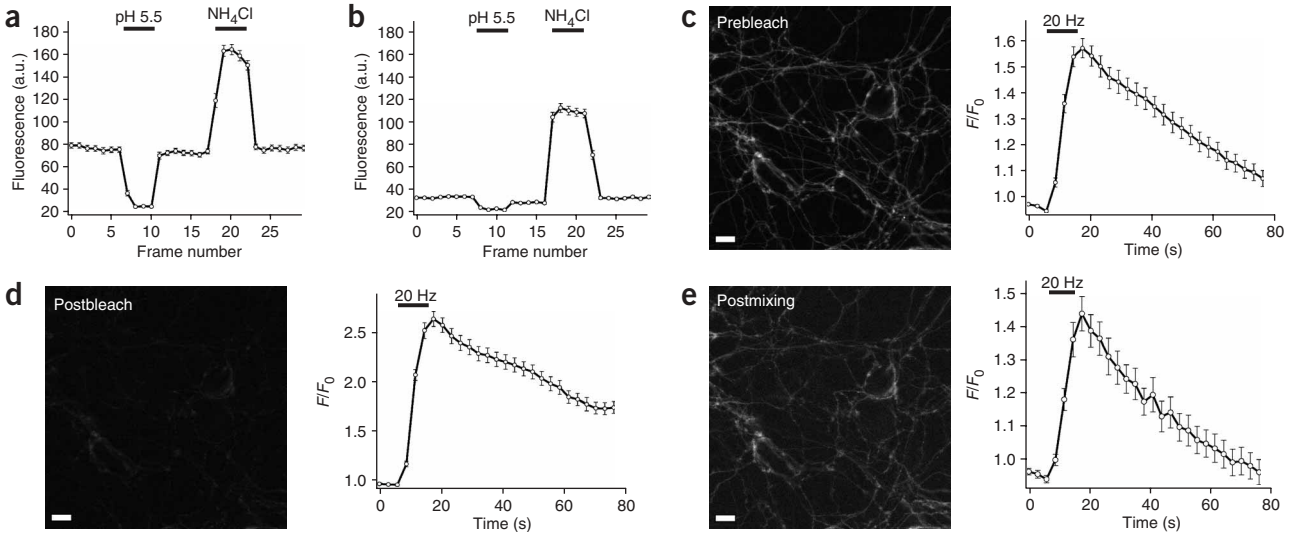

Figure 4 Nonidentity is also observed after photobleaching. (**a**,**b**) The photobleaching of plasma membrane–stranded spH-TEV occurred ten times as fast as that of quenched vesicular spH-TEV. Applying sequential pulses of an acidic solution and an ammonium chloride solution, before (**a**) and after (**b**) 90 s of repeated laser scanning at high intensity, showed that 88.9% of the unquenched plasma membrane spH-TEV pool, but only 8.5% of the quenched vesicular spH-TEV pool, was photobleached, as seen by the reduction of the fluorescence change during the acid or the ammonium pulse, respectively. Each frame is 2.9 s long. Error bars represent s.e.m. $n = 79$ and $n = 80$ boutons, respectively. (**c**) Left, image of axonal arborizations expressing spH-TEV. Right, fluorescence transients before photobleaching (200 action potentials at 20 Hz). (**d**) Left, image of axonal arborizations depicted in **c** after selective photobleaching of the plasma membrane–stranded spH-TEV pool by repetitive laser scanning at 488 nm for 90 s. Right, fluorescence transients upon stimulation (200 action potentials at 20 Hz). (**e**) Left, image of axonal arborizations depicted in **c** after mixing vesicle and plasma membrane pools of spH-TEV, by using a prolonged train of action potentials (800 action potentials at 5 Hz). Right, fluorescence transients upon stimulation (200 action potentials at 20 Hz), error bars represent s.e.m. (all conditions). Scale bar in **c**–**e**, 10 μm.

the active zone, but are internalized during another round of stimulation. Digestion would render such membrane patches fluorescently silent, thereby leading to incomplete fluorescence recovery if these patches at endocytic sites are retrieved preferentially over those freshly inserted at the release sites.

Degree of nonidentity depends on stimulus duration

If the degree of recovery reflects the amount of vesicular spH-TEV released relative to the amount of stranded spH-TEV, it should depend on the stimulus duration. Indeed, a stimulus of 200 action potentials yielded substantially more recovery (50% at 58 s after stimulus end) of the transients after digestion (**Fig. 3c**, inset). However, different degrees of recovery for differing ratios of vesicular and stranded spH-TEV may also be a consequence of a competition between cleaved and non-cleaved forms of spH-TEV for binding at sites of endocytosis. In fact, the cleaved form lacking the 27-kDa pHluorin moiety may be preferentially retrieved for steric reasons.

To test this, we sought to silence the fluorescence of the stranded pool by selective photobleaching[8], using repeated laser scanning at high intensity to minimize bleaching time and thereby any turnover by spontaneous release. By using sequential pulses of acidic and high ammonium solution, we indeed found that bleaching of unquenched stranded spH-TEV was about tenfold as effective as that of quenched vesicular spH-TEV (**Fig. 4a**,**b**). We next stimulated spH-TEV–expressing boutons ($n = 4$ experiments, >50 boutons each) with 200 action potentials at 20 Hz, before and after bleaching as well as following mixing after bleaching (with 800 action potentials at 5 Hz). Qualitatively and quantitatively, the same results were obtained as for digestion (**Fig. 4c**–**e**, **Fig. 3c** inset, and **Supplementary Fig. 2** online). This demonstrates that neither the protease treatment nor the presence of the large pHluorin moiety affects synaptobrevin recycling or rates of endocytosis.

Nonidentity is also observed for synaptotagmin-1

Is the observed nonidentity, with respect to synaptobrevin, of exo- and endocytosed vesicles specific to this protein, or are other vesicle proteins also lost after fusion? To answer this question, we constructed a chimera of a signal sequence–tagged pHluorin fused to the lumenal N terminus of synaptotagmin-1 bridged by a TEV protease cleavage site (sytpH-TEV). The sytpH-TEV chimera was properly targeted to presynaptic vesicles (**Fig. 5**) and colocalized with other presynaptic vesicle proteins (data not shown).

Electrical stimulation gave rise to stimulation-dependent fluorescence transients at synaptic boutons, indistinguishable from spH-TEV responses (**Fig. 5d**). Similar to that found for spH-TEV, acid quenching and alkalinization of the vesicular lumen with ammonium revealed that 23.9 ± 5.6% of sytpH-TEV was stranded ($n = 3$ experiments, >50 boutons each) (**Fig. 5b**). When most of the plasma membrane–stranded sytpH-TEV was silenced by protease treatment (**Fig. 5c**), stimulation produced, as expected, fluorescence transients that only partially recovered (**Fig. 5d**). After mixing stranded and vesicular pools by stimulation with 800 action potentials at 5 Hz, transients once again recovered completely in the same set of boutons (**Fig. 5d**). For both spH-TEV and sytpH-TEV, the sizes of the stranded pools were similar and the degree of recovery after digestion was the same (**Fig. 5d**) for a given stimulus protocol (here 200 action potentials at 20 Hz). Thus, the loss of vesicle proteins is a more general property of fusing synaptic vesicles.

Stranded pool size is under modulatory control

Interactions between pairs of synaptic vesicle proteins can play a role in synaptic vesicle biogenesis[25]. Synaptobrevin/VAMP-2 forms a complex on the synaptic vesicle membrane with synaptophysin-1 (ref. 26). Therefore the change in the stoichiometry of vesicular proteins by

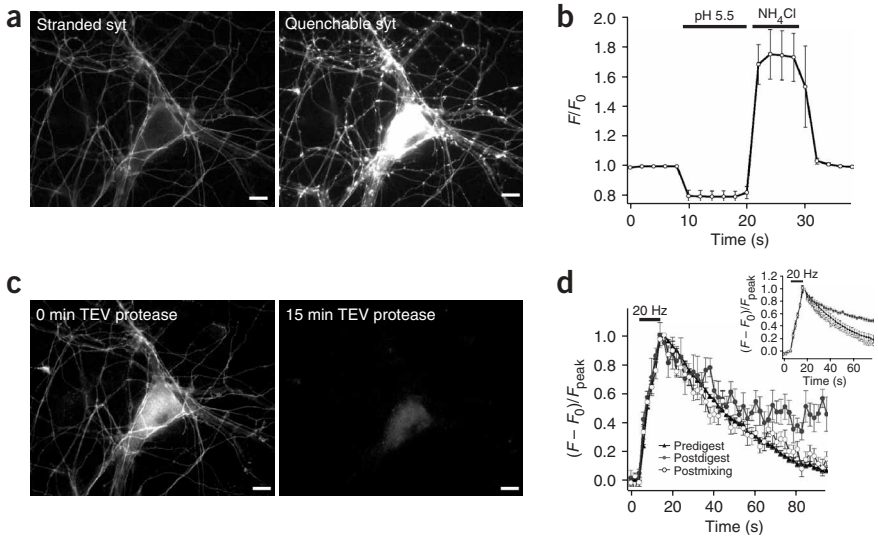

Figure 5 Nonidentity is also observed for synaptotagmin-1-TEV-pHluorin. (**a**) Images of axonal arborizations expressing sytpH-TEV, showing the fluorescence distribution of plasma membrane–stranded and vesicular sytpH-TEV. Image at left was computed by subtracting pictures before and during a pulse with acidic solution, and that at right was computed by subtracting picures during and after a pulse with ammonium chloride solution. (**b**) Fluorescence profiles of boutons during sequential pulses of acidic solution and ammonium chloride solution are similar to those of spH-TEV (error bars represent s.e.m.). (**c**) Images of axonal arborizations of **a** after 0 and 15 min of TEV protease treatment at room temperature. (**d**) Normalized sytpH-TEV fluorescence transients of boutons (shown in **a**) upon application of 200 action potentials at 20 Hz, predigest, postdigest and postmixing. The degree of incomplete recovery after digestion is the same as that seen with spH-TEV under the same conditions (inset). Scale bars in **a** and **c**, 10 μm.

synaptobrevin (or spH) overexpression might artificially introduce a membrane pool of 'missorted' synaptobrevins/spH (ref. 27). Thus, to control for a potential overexpression artefact, we cotransfected spH along with synaptophysin-mRFP (**Fig. 6a**). Synaptophysin-eGFP has successfully been used as a synaptic vesicle marker[28], so regions with overlapping green (spH-TEV) and red (synaptophysin-mRFP) fluorescence indicate the locations of presynaptic boutons. This did not abolish targeting of a substantial fraction of spH-TEV to the plasma membrane; however, it resulted in an about threefold change of the vesicular membrane–to–plasma membrane distribution ratio (percent stranded spH-TEV ± s.e.m., control 33.2 ± 0.9, + Syp 10.1 ± 0.8; $n = 3$ and 5 experiments, respectively) (**Fig. 6b**). Accordingly, the relative amplitudes of fluorescence transients upon stimulation (F/F_0) were increased (also about threefold) when synaptophysin-mRFP was coexpressed (**Fig. 6c**, left). But both the absolute fluorescence intensity of synapses during ammonium application, a measure for the total expression of spH-TEV in boutons, and the size of the absolute amplitudes after stimulation with 200 action potentials were unchanged when both synaptophysin-mRFP and spH-TEV were overexpressed (total expression levels in arbitrary units ± s.e.m. were 1,006 ± 177 in control and 905 ± 156 in + Syp; absolute amplitudes in arbitrary units ± s.e.m. were 127 ± 32 in control and 88 ± 23 in + Syp; $n = 3$ experiments for control, 5 for synaptophysin coexpression, >50 boutons each). This suggests that the number of spH-TEV copies per vesicle is similar for both conditions. Peak-normalized signals, however, revealed that the degree of recovery was slightly larger in the presence of synaptophysin-mRFP (**Fig. 6c**, right). These data suggest that the stoichiometry of proteins inside vesicles is almost independent of the relative expression levels—that is, only a certain number of 'slots' can be occupied by each protein species per vesicle. But the relative steady-state concentrations of vesicular proteins stranded in the bouton membrane are modified by the retrieval efficiency for a given protein species[29]. This also identifies vesicle formation at the bouton plasma membrane as a major sorting step in synaptic vesicle recycling and biogenesis.

Although overexpression of spH-TEV or sytpH-TEV alone obviously leads to artificially increased pools of plasma membrane–stranded proteins, the existence of a pool of a small percentage of all vesicular components at the bouton membrane may be of high functional significance. To test this more rigorously, we sought to assess the sizes of vesicular and putative plasma membrane–stranded pools in the absence of any overexpression. To this end, we used a polyclonal antibody to the ecto- or luminal domain of synaptotagmin-1 (ref. 30). Incubation of living neurons (nonpermeabilized) with this antibody at 4 °C in saline with 1 μM tetrodotoxin (TTX) and without calcium indeed yielded specific staining of synaptic boutons (**Fig. 6d**, top), albeit with weak fluorescence intensities when compared to the signals obtained with the same primary and secondary antibodies after fixation and permeabilization (**Fig. 6d**, bottom). Although we cannot fully rule out antibody uptake by spontaneous activity during the staining procedure for nonpermeabilized cells, the fluorescence intensity profiles along axons with specific staining at interconnecting axon segments (note that the feeding glial cell layer is not stained) suggest that a measurable fraction of vesicular proteins are stranded at the plasma membrane under native conditions as well. The measured levels of about 10 and 80 fluorescence arbitrary units for nonpermeabilized and permeabilized conditions (10.6 ± 0.9 arbitrary units for unpermeabilized cells, 6 images with >50 boutons each, and 83.9 ± 5.9 arbitrary units for permeabilized cells, 8 images with >50 boutons each) (**Fig. 6e**), however, may be misleading because epitope accessibility may be very different and because of some possible spontaneous activity even at 4 °C.

A 'readily retrievable pool' of vesicles?

Our data show that vesicular proteins are lost after fusion and diffuse away from sites of release. This raises the question of whether vesicular proteins after fusion freely mix with the fraction of vesicular proteins stranded at the plasma membrane, or whether the stranded proteins are actually preferentially retrieved during compensatory endocytosis. In the latter case, stranded vesicle proteins might constitute a 'readily retrievable pool' of partially preassembled structures that are preferentially endocytosed upon exocytosis.

To test this, we stimulated boutons after digestion with different numbers of action potentials and assessed the retrieval efficiencies of freshly exocytosed proteins by measuring relative recovery (that is, relative to recovery after mixing) at a time when most endocytic activity has ceased but errors due to focus or bouton drift or bleaching should still be minimal (**Fig. 7**). If stranded proteins were indeed preferentially retrieved, a plot of relative recovery versus the number of action potentials should intercept the abscissa at a positive number of action

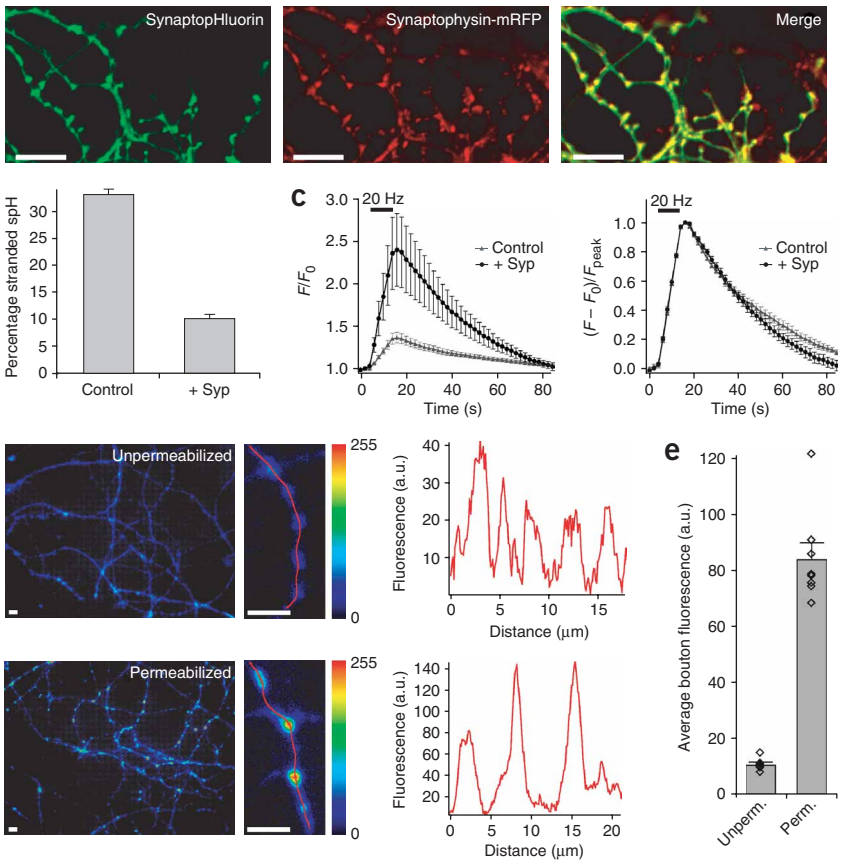

Figure 6 Stranded pool size is under modulatory control and is about 10% of total pool size under native conditions. (**a**) Images of axonal arborizations expressing spH-TEV (left) and synaptophysin-mRFP (middle). Colocalization was seen at presynaptic boutons (right). (**b**) Relative fluorescence intensities of plasma membrane–stranded spH-TEV at boutons that did not ('Control') and did ('+ Syp') overexpress synaptophysin-mRFP (along with spH-TEV), determined by sequential pulses of acidic solution or ammonium chloride solution (error bars represent s.e.m.; $P < 0.0001$). (**c**) Relative (left) and peak-normalized (right) spH-TEV fluorescence time courses at boutons that did not and did overexpress synaptophysin-mRFP (as well as spH-TEV) upon stimulation with 200 action potentials at 20 Hz ($n = 3$ and 5 experiments, respectively; >50 boutons each, error bars represent s.e.m.). (**d**) Images of axonal arborizations stained with antibodies to the ectodomain of synaptotagmin-1 without and with permeabilization (details in Methods). Detailed images for both conditions show punctate bouton staining. For nonpermeabilized cells, specific staining was also observed at the interconnecting axonal segments, better seen in the fluorescence intensity profiles (right) along the LOIs (shown as red solid lines in the detailed images). (**e**) Quantification of bouton fluorescence intensities using areas of interest of a larger set of boutons. Error bars represent s.e.m. Scale bars, 10 μm in **a**, 5 μm in **d**.

potentials. The corresponding number of vesicles would be the size of the preferentially retrieved or readily retrievable pool. Our measured relative recoveries slightly favor the existence of a preferentially retrieved pool of stranded proteins. For 40 action potentials, we found virtually no recovery after digestion (**Fig. 7**, inset), although there may have been some recovery when synaptophysin-mRFP was coexpressed (open circle in **Fig. 7**, **Supplementary Fig. 3** online). The slight slow downward trend of the signal may reflect, however, sources other than specific uptake by compensatory endocytosis, such as focus drift, bleaching, diffusional spread and so on. The finding that relative recoveries plateaued for high numbers of action potentials is in agreement with the finding that synaptic vesicle turnover reaches a maximum at about 200 action potentials (ref. 31). In addition, because of endocytosis during stimulation[32], the peak fluorescence at the end of the stimulus is increasingly underestimated for longer stimuli, leading to an underestimation of relative recovery. This may explain why we observed an even smaller recovery (albeit only slightly so) for 400 action potentials than for 200 action potentials.

DISCUSSION

We tested whether synaptic vesicles lose their identity with respect to their protein composition during stimulus-evoked exo- and endocytosis, using a fusion construct of the vSNARE synaptobrevin with the pH-sensitve GFP variant pHluorin (synapto-pHluorin). We introduced a TEV protease cleavage site between both moieties that was accessible only if spH-TEV was in the plasma membrane. We found that mostly digested molecules (that is, spH deposited on the plasma membrane before digestion) were recycled during compensatory endocytosis. This suggests that synaptic vesicles that are recycled by compensatory endocytosis lose their protein complement during exocytosis (**Figs. 1–3** and **5**), making it essential that a sorting step occurs during and maybe also after endocytosis (that is, by an endosome). Whereas cotransfection with synaptophysin-mRFP affected spH-TEV targeting to the plasma membrane, there appeared to be a small pool of stranded synaptic vesicle components under native conditions also (**Fig. 6**), from which new vesicles were retrieved preferentially (**Fig. 7**). Because the large pHluorin moiety did not affect vSNARE recycling or rates of endocytosis, this preferential endocytosis of stranded vesicle proteins cannot be attributed to sterical hindrance (**Fig. 4**).

The existence of a surface population of vesicle proteins is in agreement with previous studies that showed the expression of synaptobrevin in hippocampal neurons, which was interpreted as a result of either small inefficiencies during retrieval[16,22] or ectopic recycling during synaptogenesis[33,34] . The delivery of synaptic vesicle proteins like synaptotagmin to the plasma membrane may be important during development[30], during synaptic vesicle biogenesis and for functional maintenance of mature synapses.

Here we show that this surface-stranded pool actively participates in exo- and endocytic synaptic vesicle cycling. The pool was depleted by stimuli of more than 40 action potentials (**Fig. 7**). Notably, it has been shown that a stimulus of 40 action potentials at 20 Hz also depletes the readily releasable pool of docked vesicles, comprising about 5–10 vesicles[23,35]. Thus, the readily releasable pool of vesicles may be counterbalanced by a readily retrievable pool of preassembled endocytic structures (**Fig. 7**). Results from experiments in which both synaptophysin and spH-TEV were overexpressed, however, argue that the size of the stranded pool of vSNARES is highly overestimated in our

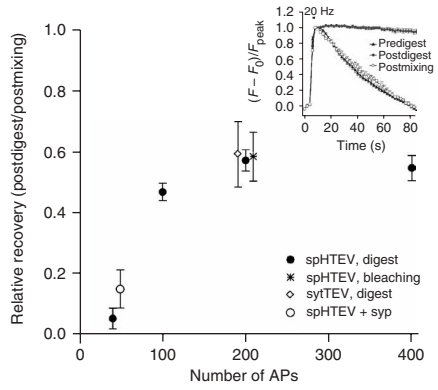

Figure 7 Stranded synaptic vesicle proteins are preferentially recycled. Postdigest or postbleach recovery (relative to postmixing recovery at $t = 58$ s after stimulus end) of bouton fluorescence transients for spH-TEV, spH-TEV + synaptophysin-RFP and sytpH-TEV, as a function of the number of action potentials applied. Inset, normalized responses for 40 action potentials at 20 Hz predigest, postdigest and postmixing ($n \geq 3$ experiments for all conditions, error bars represent s.e.m.).

measurements relying on the overexpression of spH-TEV or sytpH-TEV. On the other hand, the 'stranded' pool size measured with acidic and ammonium solution pulses (**Figs. 1** and **5**) may not be identical to the 'functional' retrievable pool size measured by determining the stimulus yielding zero recovery (**Fig. 7**). In fact, with about 200 vesicles per bouton[23], a stranded pool of 30% should correspond to 60 vesicles, whereas a functional retrievable pool of 5–10 vesicles would correspond to 2–5% fluorescence on the bouton membrane only—that is, less than our synaptotagmin immunocytochemistry data indicate to be present under native conditions (**Fig. 6d**,**e**). Thus, overexpression of one vesicle protein species may merely result in an oversupply of stranded or orphan proteins without changing the functional retrievable pool size. This is supported by our finding that coexpression of synaptophysin markedly decreased the steady-state stranded pool of spH-TEV (**Fig. 6b**), but did not affect the number of spH-TEV molecules per vesicle, nor the number of vesicles released during stimulation (**Fig. 6c**), and only slightly altered retrieval kinetics and recovery efficiency (**Fig. 7**). Likewise, in presynaptic boutons of the temperature-sensitive *Drosophila* dynamin mutant shibire, which was kept at a nonpermissive temperature to block synaptic vesicle endocytosis, dispersion of excess synaptic vesicle molecules in the plasma membrane by lateral diffusion did not alter the spatial organization of the endocytic machinery[36,37]. Thus the endocytic machinery at sites of retrieval may define the size of the functional stranded pool as opposed to that of the total stranded pool, which may also comprise excess or orphan cargo molecules.

We found that a stimulus of 40 action potentials resulted in almost complete diffusional loss of vesicle proteins after fusion; this makes for an attractive hypothesis—namely, that a small pool of readily retrievable vesicle patches exists near the active zones of small CNS synapses under native conditions. It has been shown that the rate of endocytosis is fastest for this stimulus[16]. A readily retrievable pool could nicely explain a first, fast and depletable endocytic component at synapses without having to postulate a clathrin-independent mechanism like kiss and run. Such a pool of presorted or preassembled endocytic structures could also explain the fact that the first peak of endocytic pits occurs at 10 s in the frog neuromuscular junction, a finding from the electron microscopic reconstruction of the endocytic time course at this site[10]. It has been suggested that for the stimulus of 40 action potentials, kiss and run is the dominant mechanism of vesicle retrieval[7,38]. Because molecular identity is the major hallmark of kiss and run recycling, our data argue for full collapse of all fusing synaptic vesicles during stimulation with 40 action potentials. If, however, reacidification was much faster than has been recently reported ($\sim$5 s; ref. 24), kiss and run events might add only to the noise in the rising phase of our averaged fluorescence signals (**Fig. 7**, inset) and would thus go mostly undetected. But even then, one would expect to observe a sharp decrease in the averaged fluorescence after the last action potential of the stimulus, reflecting the kiss and run events triggered by the last few action potentials. We detected no such fluorescence drop (**Fig. 7**, inset).

Our observations are best explained by a model in which synaptic vesicles fully collapse after fusion and vesicle proteins disperse in the bouton membrane and are rather slowly re-sorted at specialized sites of endocytosis, which might be located at the periphery of the bouton. Alternatively, vesicles after collapse may form raft-like patches[25,39,40] that slowly diffuse *in toto* to sites of retrieval. In fact, it has been reported[8] that after photobleaching of the membrane-stranded spH pool, single exo-endocytic events are characterized by fluorescence increases and decreases of the same size, implying that all exocytosed spH molecules of a single vesicle stay together, irrespective of whether they are retrieved fast (<1 s, kiss and run) or slowly. This is contrary to our findings of fast diffusional dispersal and preferential uptake of bleached/cleaved spH for stimuli of less than 40 action potentials.

We think, however, that our finding of fast diffusion after fusion in all directions, also observed previously[16,22], favors dispersion and free mixing of vesicular and bouton membrane components. During one exo-endocytic cycle, initially only the presorted membrane patches at these specialized sites of endocytosis would be retrieved by compensatory endocytosis, leading to the observed nonidentity of exocytic and endocytic vesicles as long as the presorted pool was not depleted—that is, for stimuli of less than 40 action potentials. For prolonged stimulation, a mixture of fast retrieval of presorted structures and slow retrieval of newly inserted vesicle components was observed, resulting in progressively slower endocytic kinetics with stronger or longer stimuli[16].

In non-neuronal cells, numerous stationary clathrin structures are often observed[19,41,42]. In presynaptic boutons, however, such clathrin structures have thus far not been detected. But spatial segregation of exocytic and endocytic sites in presynaptic boutons has been observed (see ref. 43 for review). In *Drosophila* neuromuscular junction[36,44,45], for example, components of the endocytic machinery, like dynamin and α-adaptin, are highly enriched at 'hot spots', indicating that the molecular players of the endocytic machinery are anchored at specialized sites and thereby act as spatial organizers of endocytosis. The future challenge will be to dissect the general principles of the exo- and endocytic spatial coordination and their tight temporal coupling. If it is not the exocytosed vesicle proteins themselves that trigger their own retrieval, how might this tight coupling occur? Maybe the arrival of new proteins in the periactive zone forces compensatory endocytosis of the readily retrievable pool. Alternatively, a physical link between membrane tension and endocytosis or the trigger for exocytosis—that is, a rise of intracellular calcium concentration—may couple compensatory endocytosis to exocytosis.

METHODS

Cell culture. Hippocampal neurons of the CA3/CA1 region from 1- to 3-d-old Wistar rats were prepared in a rather sparse culture ($\sim$2,000–5,000 cells per coverslip) and transfected at 4–6 days *in vitro* (DIV) by a modified calcium phosphate transfection procedure[46]. Microscopy was performed at 14–16 DIV.

Plasmid constructs. Superecliptic pHluorin-synaptobrevin-2 (synapto-pHluorin; ref. 15) was provided by G. Miesenböck (Yale University, New Haven). A DNA fragment encoding the cleavage site for recombinant TEV protease (rTEV) flanked by spacer arms (amino acid sequence SGGSGGDY DIPTTENLYFQGELKTVDAD), according to the manufacturer's recommendations (Invitrogen), was introduced into the linker region between the synaptobrevin-2 and the pHluorin moiety by polymerase chain reaction (PCR).

The synaptotagmin-1-TEV-pHluorin (sytpH) expression construct was made by first fusing the rTEV target site flanked by spacer arms (amino acid sequence DYDIPTTENLYFQGELKTVDAD) to rat synaptotagmin-1. In a second step, the cDNAs encoding the signal sequence of rat preprotachykinin and the pHluorin were fused to the amino-terminal domain of the construct[29].

Monomeric red fluorescent protein[47] was used to replace eGFP in a plasmid encoding for a GFP-tagged p38 (ref. 28; gift of A. Iliev, European Neuroscience Institute, Göttingen, Germany) to generate the synaptophysin-mRFP construct.

All constructs were cloned into a modified version of the pcDNA3 expression plasmid (Invitrogen) carrying a neuron-specific human synapsin-1 gene promoter[48] (obtained from S. Kügler, University of Göttingen, Germany) and were verified by dideoxynucleotide sequencing.

Enzymatic tag removal. Proteolytic cleavage was performed at room temperature (23 °C) by adding 60 U AcTEV protease and 1 mM dithiothreitol (Invitrogen) directly to the living neurons for 15 min. The progress of cleavage was assayed by imaging the loss of fluorescence. After digestion, cells were washed for 2 min.

Immunocytochemistry. To assess the fraction of noninternalized surface-stranded synaptotagmin-1 (syt1), live neurons were labeled with monoclonal syt1 lumenal domain antibody (mouse monoclonal, ascites, 604.4, 1:100; Synaptic Systems) at 4 °C in nominally Ca^{2+}-free solution in the presence of TTX and 4% goat serum for 1 h to allow for specific binding. Cells were washed, fixed with 4% formaldehyde (freshly prepared from paraformaldehyde) at 4 °C for 30 min, and stained with Alexa 546 secondary antibodies (1:1,000; Invitrogen).

For labeling the total pool of syt1, cells were fixed, permeabilized with 0.4% saponin (Sigma) and labeled with the primary and secondary antibodies as above. Images were acquired using equal light exposure times for both conditions.

Epifluorescence and confocal microscopy of living neurons. A modified Tyrode solution (150 mM NaCl, 4 mM KCl, 1 mM $MgCl_2$, 2 mM $CaCl_2$, 10 mM glucose, 10 mM HEPES buffer, pH 7.4) was used for all experiments unless otherwise indicated. Synaptic boutons were stimulated by electric field stimulation (platinum electrodes, 10-mm spacing, 1-ms pulses of 50 mA and alternating polarity); 10 μM 6-cyano-7-nitroquinoxaline-2,3-dione (CNQX) and 50 μM D,L-2-amino-5-phosphonovaleric acid (AP5) were added to prevent recurrent activity. Fast solution exchanges were achieved by a piezo-controlled stepper device (SF77B, Warner Instruments) using a three-barrel glass tubing. Ammonium chloride solution (pH 7.4) was prepared by substituting 50 mM NaCl in normal saline with NH_4Cl, while all other components remained unchanged. Acidic solution with a final pH of 5.5 was prepared by replacing HEPES with 2-[*N*-morpholino]ethane sulphonic acid ($pK_a = 6.1$).

In some experiments, recycling synaptic vesicles were additionally labeled with FM5-95 (Invitrogen). Cells were exposed to 10 μM FM5-95 during and for 1 min after stimulation and washed for 10 min before imaging.

Images were taken by a cooled slow-scan CCD camera (SensiCam-QE, PCO) mounted on an inverted microscope (Axiovert S100TV, Zeiss) with a 63×, 1.2 NA water-immersion objective and an eGFP filter set (DCLP 505, BP 525/50). PHluorins were excited at 470 nm with a computer-controlled monochromator (Polychrom II, Till Photonics) every 2 s for 500 ms. FM5-95 was excited at 515 nm and imaged using 565 nm dichroic and 590 nm long-pass emission filters. Photobleaching was performed by repetitive laser scanning at 488 nm for 90 s (SP2 confocal microscope, Leica).

Quantitative analysis was performed with self-written macros in Igor Pro (Wavemetrics). To avoid the bias introduced by manual selection of functional boutons, an automated detection algorithm was used. The image from the time series showing the maximal pHluorin response during stimulation was subjected to an à trous wavelet transformation with the level $k = 4$ and detection level $l_d = 1.0$ (ref. 49), resulting in a segmented mask image. Spots on mask images, each representing putative functional boutons, were identified, and only masks with areas between 4 and 20 pixels were accepted for calculating bouton fluorescence transients. All identified masks and calculated time courses were visually inspected for correspondence to individual functional boutons.

Note: Supplementary information is available on the Nature Neuroscience website.

ACKNOWLEDGMENTS

We are grateful to O. Kochubey for his assistance with data analysis, R. Nehring for advice in molecular biology, E. Neher for support, A.K. Boegle and T. Groemer for critically reading the manuscript, all lab members for fruitful discussions and M. Pilot for expert technical assistance. This work was supported by grants from the Deutsche Forschungsgemeinschaft (SFB 523, J.K.), the Human Frontier Science Project (J.K.) and the Boehringer Ingelheim Fonds (M.W.).

COMPETING INTERESTS STATEMENT

The authors declare that they have no competing financial interests.

Published online at http://www.nature.com/natureneuroscience
Reprints and permissions information is available online at http://npg.nature.com/reprintsandpermissions/

1. Heuser, J.E. & Reese, T.S. Evidence for recycling of synaptic vesicle membrane during transmitter release at the frog neuromuscular junction. *J. Cell Biol.* **57**, 315–344 (1973).
2. Cremona, O. & De Camilli, P. Synaptic vesicle endocytosis. *Curr. Opin. Neurobiol.* **7**, 323–330 (1997).
3. Brodin, L., Low, P. & Shupliakov, O. Sequential steps in clathrin-mediated synaptic vesicle endocytosis. *Curr. Opin. Neurobiol.* **10**, 312–320 (2000).
4. Brodsky, F.M., Chen, C.Y., Knuehl, C., Towler, M.C. & Wakeham, D.E. Biological basket weaving: formation and function of clathrin-coated vesicles. *Annu. Rev. Cell Dev. Biol.* **17**, 517–568 (2001).
5. Ceccarelli, B., Hurlbut, W.P. & Mauro, A. Turnover of transmitter and synaptic vesicles at the frog neuromuscular junction. *J. Cell Biol.* **57**, 499–524 (1973).
6. Koenig, J.H., Yamaoka, K. & Ikeda, K. Omega images at the active zone may be endocytotic rather than exocytotic: implications for the vesicle hypothesis of transmitter release. *Proc. Natl. Acad. Sci. USA* **95**, 12677–12682 (1998).
7. Aravanis, A.M., Pyle, J.L. & Tsien, R.W. Single synaptic vesicles fusing transiently and successively without loss of identity. *Nature* **423**, 643–647 (2003).
8. Gandhi, S.P. & Stevens, C.F. Three modes of synaptic vesicular recycling revealed by single-vesicle imaging. *Nature* **423**, 607–613 (2003).
9. Takei, K., Mundigl, O., Daniell, L. & De Camilli, P. The synaptic vesicle cycle: a single vesicle budding step involving clathrin and dynamin. *J. Cell Biol.* **133**, 1237–1250 (1996).
10. Ryan, T.A. *et al.* The kinetics of synaptic vesicle recycling measured at single presynaptic boutons. *Neuron* **11**, 713–724 (1993).
11. Ryan, T.A., Smith, S.J. & Reuter, H. The timing of synaptic vesicle endocytosis. *Proc. Natl. Acad. Sci. USA* **93**, 5567–5571 (1996).
12. Wu, L.G. & Betz, W.J. Nerve activity but not intracellular calcium determines the time course of endocytosis at the frog neuromuscular junction. *Neuron* **17**, 769–779 (1996).
13. Klingauf, J., Kavalali, E.T. & Tsien, R.W. Kinetics and regulation of fast endocytosis at hippocampal synapses. *Nature* **394**, 581–585 (1998).
14. Miesenbock, G., De Angelis, D.A. & Rothman, J.E. Visualizing secretion and synaptic transmission with pH-sensitive green fluorescent proteins. *Nature* **394**, 192–195 (1998).
15. Sankaranarayanan, S. & Ryan, T.A. Real-time measurements of vesicle-SNARE recycling in synapses of the central nervous system. *Nat. Cell Biol.* **2**, 197–204 (2000).
16. Mueller, V.J., Wienisch, M., Nehring, R.B. & Klingauf, J. Monitoring clathrin-mediated endocytosis during synaptic activity. *J. Neurosci.* **24**, 2004–2012 (2004).
17. Merrifield, C.J., Feldman, M.E., Wan, L. & Almers, W. Imaging actin and dynamin recruitment during invagination of single clathrin-coated pits. *Nat. Cell Biol.* **4**, 691–698 (2002).
18. Loerke, D., Wienisch, M., Kochubey, O. & Klingauf, J. Differential control of clathrin subunit dynamics measured with EW-FRAP microscopy. *Traffic* **6**, 918–929 (2005).
19. Miller, T.M. & Heuser, J.E. Endocytosis of synaptic vesicle membrane at the frog neuromuscular junction. *J. Cell Biol.* **98**, 685–698 (1984).
20. Sankaranarayanan, S., De Angelis, D., Rothman, J.E. & Ryan, T.A. The use of pHluorins for optical measurements of presynaptic activity. *Biophys. J.* **79**, 2199–2208 (2000).
21. Taubenblatt, P., Dedieu, J.C., Gulik-Krzywicki, T. & Morel, N. VAMP (synaptobrevin) is present in the plasma membrane of nerve terminals. *J. Cell Sci.* **112**, 3559–3567 (1999).
22. Li, Z. & Murthy, V.N. Visualizing postendocytic traffic of synaptic vesicles at hippocampal synapses. *Neuron* **31**, 593–605 (2001).
23. Schikorski, T. & Stevens, C.F. Quantitative ultrastructural analysis of hippocampal excitatory synapses. *J. Neurosci.* **17**, 5858–5867 (1997).
24. Atluri, P.P. & Ryan, T.A. The kinetics of synaptic vesicle reacidification at hippocampal nerve terminals. *J. Neurosci.* **26**, 2313–2320 (2006).

25. Thiele, C., Hannah, M.J., Fahrenholz, F. & Huttner, W.B. Cholesterol binds to synaptophysin and is required for biogenesis of synaptic vesicles. *Nat. Cell Biol.* **2**, 42–49 (2000).
26. Calakos, N. & Scheller, R.H. Vesicle-associated membrane protein and synaptophysin are associated on the synaptic vesicle. *J. Biol. Chem.* **269**, 24534–24537 (1994).
27. Pennuto, M., Bonanomi, D., Benfenati, F. & Valtorta, F. Synaptophysin I controls the targeting of VAMP2/synaptobrevin II to synaptic vesicles. *Mol. Biol. Cell* **14**, 4909–4919 (2003).
28. Kaether, C., Skehel, P. & Dotti, C.G. Axonal membrane proteins are transported in distinct carriers: a two-color video microscopy study in cultured hippocampal neurons. *Mol. Biol. Cell* **11**, 1213–1224 (2000).
29. Diril, M.K., Wienisch, M., Jung, N., Klingauf, J. & Haucke, V. Stonin 2 is an AP-2-dependent endocytic sorting adaptor for synaptotagmin internalization and recycling. *Dev. Cell* **10**, 233–244 (2006).
30. Matteoli, M., Takei, K., Perin, M.S., Sudhof, T.C. & De Camilli, P. Exo-endocytotic recycling of synaptic vesicles in developing processes of cultured hippocampal neurons. *J. Cell Biol.* **117**, 849–861 (1992).
31. Vanden Berghe, P. & Klingauf, J. Synaptic vesicles in hippocampal boutons recycle to different pools in a use-dependent fashion. *J. Physiol.* **572**, 707–720 (2006).
32. Fernandez-Alfonso, T. & Ryan, T.A. The kinetics of synaptic vesicle pool depletion at CNS synaptic terminals. *Neuron* **41**, 943–953 (2004).
33. Ahmari, S.E., Buchanan, J. & Smith, S.J. Assembly of presynaptic active zones from cytoplasmic transport packets. *Nat. Neurosci.* **3**, 445–451 (2000).
34. Sampo, B., Kaech, S., Kunz, S. & Banker, G. Two distinct mechanisms target membrane proteins to the axonal surface. *Neuron* **37**, 611–624 (2003).
35. Murthy, V.N. & Stevens, C.F. Reversal of synaptic vesicle docking at central synapses. *Nat. Neurosci.* **2**, 503–507 (1999).
36. Estes, P.S. *et al.* Traffic of dynamin within individual *Drosophila* synaptic boutons relative to compartment-specific markers. *J. Neurosci.* **16**, 5443–5456 (1996).
37. Roos, J. & Kelly, R.B. The endocytic machinery in nerve terminals surrounds sites of exocytosis. *Curr. Biol.* **9**, 1411–1414 (1999).
38. Pyle, J.L., Kavalali, E.T., Piedras-Renteria, E.S. & Tsien, R.W. Rapid reuse of readily releasable pool vesicles at hippocampal synapses. *Neuron* **28**, 221–231 (2000).
39. Martin, T.F. Racing lipid rafts for synaptic-vesicle formation. *Nat. Cell Biol.* **2**, E9–11 (2000).
40. Willig, K.I., Rizzoli, S.O., Westphal, V., Jahn, R. & Hell, S.W. STED microscopy reveals that synaptotagmin remains clustered after synaptic vesicle exocytosis. *Nature* **440**, 935–939 (2006).
41. Gaidarov, I., Santini, F., Warren, R.A. & Keen, J.H. Spatial control of coated-pit dynamics in living cells. *Nat. Cell Biol.* **1**, 1–7 (1999).
42. Kirchhausen, T. Clathrin. *Annu. Rev. Biochem.* **69**, 699–727 (2000).
43. Gundelfinger, E.D., Kessels, M.M. & Qualmann, B. Temporal and spatial coordination of exocytosis and endocytosis. *Nat. Rev. Mol. Cell Biol.* **4**, 127–139 (2003).
44. Gonzalez-Gaitan, M. & Jackle, H. Role of *Drosophila* alpha-adaptin in presynaptic vesicle recycling. *Cell* **88**, 767–776 (1997).
45. Roos, J. & Kelly, R.B. Dap160, a neural-specific Eps15 homology and multiple SH3 domain-containing protein that interacts with *Drosophila* dynamin. *J. Biol. Chem.* **273**, 19108–19119 (1998).
46. Threadgill, R., Bobb, K. & Ghosh, A. Regulation of dendritic growth and remodeling by Rho, Rac, and Cdc42. *Neuron* **19**, 625–634 (1997).
47. Campbell, R.E. *et al.* A monomeric red fluorescent protein. *Proc. Natl. Acad. Sci. USA* **99**, 7877–7882 (2002).
48. Kugler, S. *et al.* Neuron-specific expression of therapeutic proteins: evaluation of different cellular promoters in recombinant adenoviral vectors. *Mol. Cell. Neurosci.* **17**, 78–96 (2001).
49. Olivo-Marin, J.-C. Extraction of spots in biological images using multiscale products. *Pattern Recognit.* **35**, 1989–1996 (2002).